Fermilab–Pub–95/362-T
UM–TH–95–26
hep-ph/9512264

Angular Correlations in Top Quark Pair Production and Decay at Hadron Colliders

Gregory Mahlon*

Department of Physics, University of Michigan

500 E. University Ave., Ann Arbor, MI 48109

Stephen Parke†

Fermi National Accelerator Laboratory

P.O. Box 500, Batavia, IL 60510

(December 8, 1995)

Abstract

We show how to observe sizable angular correlations between the decay products of the top quark and those of the anti-top quark in top quark pair production and decay at hadron colliders. These correlations result from the large asymmetry in the rate for producing like-spin versus unlike-spin top quark pairs provided the appropriate spin axes are used. The effects of new physics at production or decay on these correlations are briefly discussed.

14.65.Ha, 13.88.+e

Typeset using REVTEX

I. INTRODUCTION

Now that CDF [1] and D0 [2] have observed the top quark (t) and reported mass values of $176 \pm 8 \pm 10$ GeV and $199^{+19}_{-21} \pm 22$ GeV respectively, it is important to reconsider what other quantities associated with top-antitop ($t\bar{t}$) production may be measured with the data to be collected at both the Tevatron and LHC. One interesting avenue of investigation consists of a study of the angular correlations between the decay products of the top quark and those of the anti-top quark. For a top quark mass in the range reported by experiments, it has been known for some time that the top quark will decay before hadronization takes place [3]. Therefore, the angular correlations in the top quark decay contain information on the spin of the top quark. If the production mechanism of the $t\bar{t}$ pair correlates the spins of the top and anti-top, then this correlation will lead to angular correlations between their decay products.

The study of angular correlations in $t\bar{t}$ production was pioneered by Barger, Ohnemus and Phillips [4]. These authors concluded that the decay product angular correlations induced by the spin correlations of top and anti-top were small when summed over all events. Kane *et. al.* [5,6] reached similar conclusions in their papers on the transverse polarization of top quarks induced by QCD loop effects. Since then many authors have found similar results for hadron colliders [7–10]. Other studies have addressed this issue at lepton colliders [11–14].

In this paper we exploit the fact that, even though the net polarization of top quark pairs is very small, there is a very large asymmetry in the rate for producing the like-spin versus unlike-spin top quark pairs at hadron colliders if the appropriate spin axes are chosen. Barger *et. al.* [4] used this fact to explain the small global correlation features of top quark production at the Tevatron, while Schmidt and Peskin [7] used this asymmetry to study CP violation near threshold at the LHC and SSC. However, this asymmetry in the number of like- to unlike-spin top pairs is true at any hadron collider independent of whether the top quarks are produced via gluon-gluon fusion or quark-antiquark annihilation both near and far from threshold. To use the spin correlation induced by this asymmetry, we make simple

cuts on the top (anti-top) quark side of an event to select a given spin for the top (anti-top) quark, and then observe specific correlations in the decay products on the anti-top (top) quark side of the event. These correlations are large and can be observed in the $t\bar{t}$ events at both the Tevatron and the LHC.

Our discussion is organized as follows. In Sec. II we examine the amplitudes for $q\bar{q} \to t\bar{t}$ and $gg \to t\bar{t}$ with polarized top quark production. Our emphasis will be upon the excess of unlike-spin $t\bar{t}$ pairs at the Tevatron and the excess of like-spin $t\bar{t}$ pairs at the LHC. The form of the relevant amplitudes using an appropriate choice of the spin axes and the relative parton luminosities at the two machines combine to produce these asymmetries. A description of the spinor helicity basis for massive particles used in this section appears in the Appendix, and is presented here because of its broad applicability. In Sec. III we review the decay of a polarized top quark. In Sec. IV we describe how to observe the angular correlations arising from the production and decay of $t\bar{t}$ pairs. We briefly discuss some possibilities for new physics effects in Sec. V. Finally, Sec. VI contains the conclusions.

II. POLARIZED $t\bar{t}$ PRODUCTION

In this section we present the squares of the helicity amplitudes for polarized $t\bar{t}$ production for both quark-antiquark ($q\bar{q}$) and gluon-gluon (gg) initial states. The expressions given below have been summed over the spins of the initial partons, as well as the colors of both the initial and final states. Spin- and color-averaging factors have *not* been included. We represent the momentum of the particle by its symbol and decompose the top quark (anti-top quark) momentum into a sum of two massless momenta, $t = t_1 + t_2$ ($\bar{t} = \bar{t}_1 + \bar{t}_2$), such that in rest frame of the top quark (anti-top quark) the spatial momentum of t_1 ($\bar{t}_1$) defines the spin axis for the top (anti-top) quark (see the appendix for details).

For $q\bar{q} \to t\bar{t}$, we have [6]

$$\sum_{\uparrow\uparrow,\,\downarrow\downarrow} |\mathcal{M}(q\bar{q} \to t\bar{t})|^2 = \frac{16g^4}{(2q\cdot\bar{q})^2}\Big[(2q\cdot t_1)(2\bar{q}\cdot\bar{t}_2) + (2q\cdot\bar{t}_1)(2\bar{q}\cdot t_2) + \frac{1}{m_t^2}\,\mathrm{Tr}\,(q\,t_1\,t_2\,\bar{q}\,\bar{t}_2\,\bar{t}_1)\Big] + (\,q \leftrightarrow \bar{q}\,) \tag{2.1}$$

for the production of like-spin $t\bar{t}$ pairs, and

$$\sum_{\uparrow\downarrow,\,\downarrow\uparrow} |\mathcal{M}(q\bar{q} \to t\bar{t})|^2 = \frac{16g^4}{(2q\cdot\bar{q})^2}\Big[(2q\cdot t_1)(2\bar{q}\cdot\bar{t}_1) + (2q\cdot\bar{t}_2)(2\bar{q}\cdot t_2) + \frac{1}{m_t^2}\,\mathrm{Tr}\,(q\,t_1\,t_2\,\bar{q}\,\bar{t}_1\,\bar{t}_2\,)\Big] + (\,q \leftrightarrow \bar{q}\,) \tag{2.2}$$

for unlike-spin pairs [15]. Note that the sum of (2.1) and (2.2) does not depend on the decomposition of the quark momenta.

The following expressions hold for initial state gluons [6,8]:

$$\sum_{\uparrow\uparrow,\,\downarrow\downarrow} |\mathcal{M}(gg \to t\bar{t})|^2 = \frac{4}{3}g^4\left\{\frac{4}{(t\cdot g_1)^2} - \frac{1}{(t\cdot g_1)(t\cdot g_2)} + \frac{4}{(t\cdot g_2)^2}\right\}\Big\{m_t^2\,[(2t_1\cdot\bar{t}_1) + (2t_2\cdot\bar{t}_2)] - \frac{\mathrm{Tr}\,(g_1\,t\,g_2\,\bar{t})}{(2g_1\cdot g_2)^2}\Big[(2g_1\cdot t_1)(2g_2\cdot\bar{t}_2) + (2g_1\cdot\bar{t}_1)(2g_2\cdot t_2) + \frac{1}{m_t^2}\,\mathrm{Tr}\,(g_1\,t_1\,t_2\,g_2\,\bar{t}_2\,\bar{t}_1)\Big]\Big\} + (\,g_1 \leftrightarrow g_2\,), \tag{2.3}$$

and

$$\sum_{\uparrow\downarrow,\,\downarrow\uparrow} |\mathcal{M}(gg \to t\bar{t})|^2 = \frac{4}{3}g^4\left\{\frac{4}{(t\cdot g_1)^2} - \frac{1}{(t\cdot g_1)(t\cdot g_2)} + \frac{4}{(t\cdot g_2)^2}\right\}\Big\{m_t^2\Big[(2t_1\cdot\bar{t}_2) + (2\bar{t}_1\cdot t_2)\Big] - \frac{\mathrm{Tr}\,(g_1\,t\,g_2\,\bar{t})}{(2g_1\cdot g_2)^2}\Big[(2g_1\cdot t_1)(2g_2\cdot\bar{t}_1) + (2g_1\cdot\bar{t}_2)(2g_2\cdot t_2) + \frac{1}{m_t^2}\,\mathrm{Tr}\,(g_1\,t_1\,t_2\,g_2\,\bar{t}_1\,\bar{t}_2)\Big]\Big\} + (\,g_1 \leftrightarrow g_2\,). \tag{2.4}$$

As presented, Eqs. (2.1)–(2.4) are valid for arbitrary choices of the axes along which the t and $\bar{t}$ spins are decomposed. However, all choices are not equally effective for extracting the

correlations at hadron colliders. In fact, the same choice may not be ideal for all colliders. We shall now describe two different bases, one of which turns out to be well-suited to studies at the Tevatron, while the other is useful at both the LHC and Tevatron.

The first basis we consider is what we will refer to as the "beamline" basis. It utilizes the spin axes p_L for the top quark and p_R for the anti-top quark (*i.e.* $t_1 \propto p_L$ and $\bar{t}_1 \propto p_R$ in eqs. (2.1)–(2.4)), where p_L and p_R are light-like vectors parallel to the left and right moving beams, respectively [16]. Fortunately, the amplitude combinations we are considering are symmetric under the interchange of the initial parton momenta; therefore, it is not necessary to determine the identity of each initial parton. Furthermore, this particular basis provides a frame-independent decomposition into like- and unlike-spin pairs. We work in the zero momentum frame of the initial parton pair, where we may describe the top pair production cross section in terms of the scattering angle θ^* between the top quark and the left moving beam, and the speed β of the top quark. For the $q\bar{q}$ initial state we find

$$\sum_{\uparrow\uparrow,\,\downarrow\downarrow} |\mathcal{M}(q\bar{q} \to t\bar{t})|^2 = 8g^4 \, \frac{\beta^2(1-\beta^2)\sin^2\theta^*}{(1-\beta\cos\theta^*)^2}, \tag{2.5}$$

$$\sum_{\uparrow\downarrow,\,\downarrow\uparrow} |\mathcal{M}(q\bar{q} \to t\bar{t})|^2 = 8g^4 \left[\, 1 + \frac{(1-\beta\cos\theta^*-\beta^2\sin^2\theta^*)^2}{(1-\beta\cos\theta^*)^2}\right]. \tag{2.6}$$

Notice the factor $\beta^2(1-\beta^2)$ in the like-spin pair amplitude (2.5). It supplies suppression of this component for both small and large values of β. In contrast, the unlike-spin pair amplitude (2.6) contains a contribution which is independent of β.

For the gg initial state we define the common spin-independent angular factor

$$\mathcal{Y}(\beta, \cos\theta^*) \equiv \frac{7 + 9\beta^2\cos^2\theta^*}{(1-\beta^2\cos^2\theta^*)^2}, \tag{2.7}$$

in terms of which we have

$$\sum_{\uparrow\uparrow,\,\downarrow\downarrow} |\mathcal{M}(gg \to t\bar{t})|^2 = \frac{16}{3} g^4 \, \mathcal{Y}(\beta, \cos\theta^*) \times(1-\beta^2)\left[\, 1 + \beta^2\cos^2\theta^* + 2\beta^3\sin^2\theta^* \, \frac{(\beta - \cos\theta^*)}{(1-\beta\cos\theta^*)^2}\right], \tag{2.8}$$

$$\sum_{\uparrow\downarrow,\ \downarrow\uparrow} |\mathcal{M}(gg \to t\bar{t})|^2 = \frac{16}{3} g^4\, \mathcal{Y}(\beta, \cos\theta^*) \times \beta^2 \sin^2\theta^* \left[\ 1 + \frac{(1-\beta^2)^2 + (1 - \beta\cos\theta^* - \beta^2\sin^2\theta^*)^2}{(1-\beta\cos\theta^*)^2}\right]. \quad (2.9)$$

Eq. (2.8) shows that the like-spin pairs coming from gluon-gluon fusion will be suppressed for large β, while (2.9) tells us that unlike-spin pairs are disfavored at low β.

The other basis we wish to discuss is built upon the helicities of the t and $\bar{t}$. The helicity of a massive particle is a frame-dependent concept, so the decomposition into like- and unlike-helicity pairs will depend upon which frame is used. We choose to measure the helicities of the top and anti-top quarks in the zero momentum frame of the initial parton pair. For the $q\bar{q}$ initial state we find

$$\sum_{LL,\ RR} |\mathcal{M}(q\bar{q} \to t\bar{t})|^2 = 8g^4\ (1-\beta^2)\sin^2\theta^*, \quad (2.10)$$

$$\sum_{LR,\ RL} |\mathcal{M}(q\bar{q} \to t\bar{t})|^2 = 8g^4\ (1+\cos^2\theta^*). \quad (2.11)$$

We see from (2.10) that in the high energy limit ($\beta \to 1$), the production of like-helicity $t\bar{t}$ pairs is suppressed.

The expressions involving initial state gluons are only slightly more complex:

$$\sum_{LL,\ RR} |\mathcal{M}(gg \to t\bar{t})|^2 = \frac{16}{3} g^4\ \mathcal{Y}(\beta, \cos\theta^*)\ (1-\beta^2)(1+\beta^2+\beta^2\sin^4\theta^*), \quad (2.12)$$

$$\sum_{LR,\ RL} |\mathcal{M}(gg \to t\bar{t})|^2 = \frac{16}{3} g^4\ \mathcal{Y}(\beta, \cos\theta^*)\ \beta^2\sin^2\theta^*(1+\cos^2\theta^*). \quad (2.13)$$

Once again, we see suppression of like-helicity $t\bar{t}$ pairs in the high energy limit. However, we note that for low energies, unlike-helicity pair production is suppressed relative to the production of like-helicity pairs by a factor of β^2.

The difference in the β dependence of these squared matrix elements is such that at nearly all hadron colliders, the $t\bar{t}$ pairs are produced with one or other of the spin configurations dominating the cross section. In Fig. 1 we show the β distributions for 175 GeV top quarks produced at the Tevatron and the LHC [17]. The breakdown of the total $t\bar{t}$ cross section into like- and unlike-spin pairs as a function of the $t\bar{t}$ invariant mass is given in Figs. 2 and 3

for the Tevatron using the "beamline" and helicity bases respectively. In the "beamline" basis 80% of the $t\bar{t}$ pairs have unlike spins, while in the helicity basis 67% of the $t\bar{t}$ pairs have unlike helicities [18]. Fig 4 is the same breakdown at the LHC using the helicity basis, where 67% of the $t\bar{t}$ pairs have like helicities [19]. These asymmetries may be understood in terms of the amplitudes (2.5)–(2.13) and relative parton luminosities at the two machines. It is well-known that $t\bar{t}$ production at the Tevatron is dominated by the $q\bar{q}$ initial state. Furthermore, Eq. (2.5) tells us that the production of like-spin $t\bar{t}$ pairs in the "beamline" basis from a $q\bar{q}$ initial state is disfavored. Consequently, most of the $t\bar{t}$ pairs produced at the Tevatron have unlike spins in this description. Similar considerations may be applied to understand the production asymmetries in terms of the helicity basis at both machines.

Since the β and θ^* dependence is different for different spin configurations, we may ask if it is possible to devise a set of cuts which would increase the purity of the dominant spin configuration. For the Tevatron using the "beamline" basis, this turns out to be difficult. We have found that in order to increase the fraction of unlike-spin $t\bar{t}$ pairs by more than a percent or two, it is necessary to apply such stringent cuts that the statistics are reduced by a factor of 10 or more. Fortunately, 80% purity is already sufficiently good to render the correlations we wish to consider visible (see Sec. IV). On the other hand, using the helicity basis at the Tevatron and requiring $M_{t\bar{t}}$ to be larger than some value will improve the unlike-helicity purity of the sample. In Fig. 5 we show how such a cut affects the fraction of unlike-helicity pairs, as well as the fraction of the total $t\bar{t}$ sample retained by such a cut. Using this basis with the cut $M_{t\bar{t}} > 450$ GeV increases the unlike-helicity fraction to 74%, while retaining 47% of the data sample.

It may also be desirable at the LHC to impose a cut on $M_{t\bar{t}}$. Recall that Eqs. (2.12) and (2.13) predict that for low values of β, mostly like-helicity pairs are produced, while for high values of β, mostly unlike-helicity pairs are produced. This feature is clearly visible in Fig. 4: in the 800–900 GeV region, the like- and unlike-helicity contributions from gg become equal. Thus, it is reasonable to consider selecting events with $M_{t\bar{t}}$ less than some maximum value. In Fig. 6 we show how such a cut affects the fraction of like-helicity pairs,

as well as the fraction of the total $t\bar{t}$ sample retained by such a cut. For example, if we impose the cut $M_{t\bar{t}} < 500$ GeV, we increase the like-helicity fraction to 78%, while retaining 45% of the data sample.

Lastly, all of the above fractions depend only weakly upon the value of the top quark mass, varying by only a few percent over the range 150 GeV $< m_t <$ 200 GeV.

III. POLARIZED TOP QUARK DECAY

Because of its extremely short lifetime, the top quark decays before it hadronizes, imparting its spin information to its decay products. For a 175 GeV top quark the total decay width is 1.6 GeV [3]. The squared matrix element for the complete decay chain is rather simple, considering the three-body final state. Again we decompose the top quark momentum into two massless momenta, $t = t_1 + t_2$, such that the spatial momentum of t_1 defines the spin axis in the top quark rest frame. For a top quark (t) decaying into a b-quark (b), positron ($\bar{e}$) and neutrino (ν), we obtain

$$|\mathcal{M}_{\uparrow}(t \to b\bar{e}\nu_e)|^2 = \frac{g_w^4 (2\nu \cdot b)(2\bar{e} \cdot t_2)}{(2\nu \cdot \bar{e} - M_W^2)^2 + M_W^2 \Gamma_W^2}, \tag{3.1}$$

$$|\mathcal{M}_{\downarrow}(t \to b\bar{e}\nu_e)|^2 = \frac{g_w^4 (2\nu \cdot b)(2\bar{e} \cdot t_1)}{(2\nu \cdot \bar{e} - M_W^2)^2 + M_W^2 \Gamma_W^2}. \tag{3.2}$$

For the hadronic decay of the top quark, $t \to b\,\bar{d}\,u$, one should replace the $\bar{e}$ with $\bar{d}$ and ν with u in the above expressions.

The differential decay rates in the rest frame of the decaying particle may be parameterized as

$$\frac{1}{\Gamma}\frac{d\Gamma}{d(\cos\theta_i)} = \frac{1 + \alpha_i \cos\theta_i}{2} \tag{3.3}$$

where θ_i is the angle between the chosen spin axis and the direction of motion of the ith decay product, $i = b$, $\bar{e}$, or ν (alternatively b, $\bar{d}$ or u). The correlation coefficient α_i may be computed from the matrix elements (3.1)–(3.2), see Ref. [11]. For a spin-up top quark the results are given in Table I, and plotted in Fig. 7. The spin-down top quark has correlation

coefficients opposite in sign to the spin-up case, whereas for the anti-top quark the correlation coefficients for spin-up (spin-down) equal the coefficients for the top quark with spin-down (spin-up). For $m_t = 175$ GeV the values of $\alpha_{\bar{e}}$, α_ν and α_b for a spin-up top quark are 1, -0.31, and -0.41 respectively.

These correlations can be used to determine probabilistically whether the top quark is spin-up or spin-down. For the ith decay product, if $\cos\theta_i > y$ then the probability that the top quark had spin-up, $P_\uparrow$, is given by

$$[2 + \alpha_i(1+y)]/4. \tag{3.4}$$

In the rest frame of the W-boson it is well-known that the correlation of the angle, $\theta^\dagger$, between the charged lepton (or down-type quark) and the b-quark direction is given by

$$\frac{1}{\Gamma}\frac{d\Gamma}{d(\cos\theta^\dagger)} = \frac{3}{4}\frac{m_t^2\sin^2\theta^\dagger + m_W^2(1+\cos\theta^\dagger)^2}{m_t^2+2m_W^2}, \tag{3.5}$$

reflecting the relative rate of longitudinal to transverse W-bosons in top decay of m_t^2 to $2m_W^2$. This correlation can be used to distinguish the d-type quark from the u-type quark in hadronic top quark decays. If we choose events such that one of the jets has $\cos\theta^\dagger > z$, then the probability that this jet originates from a d-type quark, P_d, is

$$\frac{m_t^2(2-z-z^2) + m_W^2(7+4z+z^2)}{2\,[m_t^2(2-z-z^2) + m_W^2(4+z+z^2)]}. \tag{3.6}$$

In Fig. 8 we have plotted all the angular correlations for a spin up top quark decay.

IV. CORRELATIONS IN $t\bar{t}$ PRODUCTION AND DECAY

In this section we put together the spin correlations induced by production, Sec. II, and the polarized decays, Sec. III. For the ith decay product of the top quark with angle θ_i to the spin axis of the top quark in the top rest frame and the $\bar{\imath}$th decay product of the anti-top quark with angle $\theta_{\bar{\imath}}$ to the spin axis of the anti-top quark in the anti-top rest frame, the correlation is given by

$$\frac{1}{\sigma}\,\frac{d^2\sigma}{d(\cos\theta_i)\,d(\cos\theta_{\bar{i}})} = \frac{1+\kappa\cos\theta_i\cos\theta_{\bar{i}}}{4}, \tag{4.1}$$

where

$$\kappa = (1-2P_X)\,\alpha_i\alpha_{\bar{i}} \tag{4.2}$$

and P_X is the fractional purity of the unlike-spin component of the sample of $t\bar{t}$ events. If both the top and anti-top quark decayed spherically in their respective rest frames [20], then the right hand side of eqn (4.1) would be simply $\frac{1}{4}$. Therefore, the contribution $\frac{1}{4}\kappa\cos\theta_i\cos\theta_{\bar{i}}$ is induced by the spin correlations of the $t\bar{t}$ pair.

The strategy to observe these angular correlations in top production at hadron colliders is to select a sample of $t\bar{t}$ pairs which have a high asymmetry in the number of like-spin to unlike-spin pairs, *i.e.* dominated by unlike-spin pairs for the Tevatron or like-helicity pairs for the LHC. Then, we choose those events for which the top quark has a given spin and look to see what the correlations of the decay products are for the anti-top quark or vice versa. At the Tevatron if the top quark had spin up, for example, then the anti-top quark should have spin down, while at the LHC, if the top quark has right helicity, then the anti-top quark should also have right helicity.

Suppose we choose those events for which the ith decay product on the top quark side of the event has an angle θ_i in the top rest frame with respect to the axis defining the top quark spin such that $\cos\theta_i > y$. Then, this top quark decay has a probability $P_\uparrow$, given by Eq. (3.4), of coming from a spin up top. Furthermore, on the anti-top quark side of the event, the α determining the angular correlation of the $\bar{i}$th decay product in Eq. (3.3) is given by

$$(1-2P_X)(2P_\uparrow - 1)\alpha_{\bar{i}}. \tag{4.3}$$

If we can only determine the identity of the $\bar{i}$th decay product probabilistically, as in the case of the d-type quark in hadronic decays, then $\alpha_{\bar{i}}$ in the above expression is replaced by

$$P_d\alpha_d \;+\; (1-P_d)\alpha_{\bar{u}}, \tag{4.4}$$

where P_d is given by Eq. (3.6).

To demonstrate these correlations we choose the $\cos\theta_i$ cut, which is used to distinguish spin up from spin down, to be at zero. This divides the data sample into two sets which we call spin "up" and spin "down". On the other side of the event we can compare the angular distributions between these two data sets. Since the charged lepton has the largest correlation to the spin direction of the quark or anti-quark, it is natural to use this particle to distinguish spin up from down. Requiring $\cos\theta > 0$ for the charged lepton yields a probability of 75% that it came from a spin up quark, *i.e.* $P_\uparrow = 0.75$. If we tighten this cut to $\cos\theta > 0.5$, then $P_\uparrow = 0.875$, thus increasing the correlations by 50%, with a factor of two loss in statistics. For dilepton events, the correlations on the other side of the event which we can study are between the charged lepton or the b-quark and the spin axis, assuming that the neutrino momenta can be determined. In the charged lepton plus four jet channel we can look at the correlations between the *"d"*-type quark or the b-quark and the spin axis. Here the *"d"*-type quark is defined as that jet which is closest to the b-quark direction in the W-boson rest frame. This allows us to include all events and is effectively a $\cos\theta^\dagger > 0$ cut. The probability that this jet comes from a (real) d-type quark is given by eqn (3.6), and equals 61% for 175 GeV top quarks. One further possibility is to look at the correlation between the b-quark and the $\bar{b}$-quark for all the double-tagged $t\bar{t}$ events, which may be done in a similar manner.

We have performed a first-pass monte carlo study of these effects at the parton level without any hadronization or jet energy smearing effects included. However, we expect these effects to be small. Also, we have used the known neutrino momenta to determine the momenta of the top quarks and hence the appropriate angles in the top quark rest frames. Studies by CDF [21] demonstrate that even in dilepton events, because of the mass constraints on the top quarks and W-bosons, the neutrino momenta can be determined to better than 10%. A further complication is the combinatoric background associated with assigning particles to the wrong top quark decay. All of these effects would need to be included in a full study of these phenomena, and would result in a reduction of the

correlations determined below.

We selected a $t\bar{t}$ sample for both the Tevatron and the LHC using the following minimal cuts on the transverse momenta, p_T, and pseudo-rapidities, η, of all final state particles: for the Tevatron we required

$$p_T > 15 \text{ GeV}, \quad |\eta| < 2, \tag{4.5}$$

while for the LHC we imposed

$$p_T > 20 \text{ GeV}, \quad |\eta| < 3. \tag{4.6}$$

No further cuts in $M_{t\bar{t}}$ or θ^* were made to increase the spin asymmetry. The monte carlo generated events with the full spin correlations using the Kleiss and Stirling [22] matrix elements squared. The events from this $t\bar{t}$ sample were analyzed as discussed in the previous paragraph, using the $\cos\theta_i > 0$ selection criteria to divide the sample into two data sets. In Figs. 9–12 we compare the results for four different correlations in each of the following three cases: the "beamline" basis at the Tevatron, the helicity basis at the Tevatron, and the helicity basis at the LHC. The correlations studied were the charged lepton of one of top quarks versus the charged lepton, Fig. 9, the *"d"*-type quark, Fig. 10, or the b-quark in the other top quark decay, Fig. 11, as well as the correlations between the two b-quarks in the $t\bar{t}$ sample, Fig. 12. For each of the particles at each of the machines we show the angular distributions of both the spin-"up" and spin-"down" data sets using the full spin-correlated matrix element squared with the minimal cuts.

These plots should be viewed in the light of the following two observations. First, if we produce data sets using the minimal cuts but allow both top quarks to decay spherically in their respective rest frames [20], we find that the resulting two curves are identical and equal to the average of the two curves shown. Hence, the difference between the plotted curves comes from the spin correlations induced in the production of the $t\bar{t}$ pair. Second, in the absence of the minimal cuts, the curves in Figs. 9–12 would be straight lines going through $(0.0, 0.5)$, with slopes easily calculable from Eq. (4.3), see Table II. For the "beamline"

basis at the Tevatron, the p_T and η cuts are approximately equally important in distorting the shape of these curves, with the most pronounced effects around $\cos\theta = 1$. If we relax these cuts to $p_T > 10$ GeV and $|\eta| < 3$, then these curves become nearly equal to the straight lines of the no cut case, except very close to $\cos\theta = 1$. For the helicity basis at the Tevatron and the LHC, the η cut plays only a minor role: for values greater than or equal to 2, this cut has essentially no effect. It is the p_T cut which is mainly responsible for the distortion of these curves from the ideal straight lines. The reason that the LHC shows a larger distortion than the Tevatron is the we have used a higher p_T cut. Although the center of mass energy at the LHC is seven times higher than at the Tevatron, top quarks produced at the LHC have on average only 10–20% higher p_T. Therefore, the same p_T cut has nearly the same effect on the correlations at both machines. For p_T cuts very much above 20 GeV, the distortions become unacceptably large, and the two curves are forced closer and closer together.

After sufficient $t\bar{t}$ events have been collected by the Tevatron or the LHC, the difference between the "up" and "down" data sets could be enhanced by making extra cuts to increase the spin asymmetry and/or tightening the selection criteria on what we have have called spin "up" and "down" top quarks.

V. SIGNATURES OF NEW PHYSICS

In this section we briefly discuss the effects of new physics on the correlations examined in the previous section. Hill and Parke [23] have proposed that the production of top pairs at hadron colliders could be affected by a new vector particle associated with top-color. Such a resonance would appear in the angular correlations for top pair production by changing the relative mixture of $q\bar{q}$ to gg initiated production of top quarks, and by distorting the zero momentum frame speed, β, for the $q\bar{q}$ component. At the Tevatron both of these effects would increase the LR+RL helicity component in top pair production so as to increase the correlations discussed in the previous section. Since the $q\bar{q}$ component at the LHC is a small

fraction of the total cross section, small changes in this component will be difficult to see.

Eichten and Lane [24] have discussed the effects of a techni-eta in two scale technicolor on top quark pair production at hadron colliders. Since the production of top pairs via a scalar or pseudoscalar goes exclusively into the LL+RR helicity state, the effect at the Tevatron of such a resonance is to reduce the correlations discussed in this paper. If the techni-eta has a mass just above the top pair threshold the charged leptons in the dilepton events will tend to be in the same hemisphere instead of in opposite hemispheres. At the LHC such a resonance would enhance the correlations produced by the Standard Model gg component.

On the decay end, new physics such as a charged Higgs decay of top would also affect these correlations. The correlation coefficients α for the decay $t \to bjj$ via a charged Higgs have values of $\alpha_b = 1.0$ and $\alpha_j = (-\xi^2 + 1 + 2\xi \ln \xi)/(\xi - 1)^2$, where $\xi = m_t^2/m_H^2$. As a result, a deviation in the standard model correlations in the W plus four jet sample of top pair production could be observed if the branching fraction for top into charged Higgs plus b-quark is large enough.

VI. CONCLUSIONS

We have described a method whereby the angular correlations between the top and anti-top decay products could be observed at a hadron collider. Our discussion is based upon the asymmetry in the number of like-spin to unlike-spin $t\bar{t}$ pairs produced at any hadron collider. When the production is dominated by quark-antiquark annihilation, there will be an excess in the number of unlike-spin $t\bar{t}$ pairs using the "beamline" basis and unlike-helicity pairs using the helicity basis. On the other hand, when gluon-gluon fusion dominates the production, there will be an excess of like-helicity pairs. The size of these excesses may be enhanced by applying a cut on any variable that selects events in a restricted β region in the zero momentum frame of the $t\bar{t}$ pair. The spin of a given top quark may be determined probabilistically by considering the angle between the direction of motion of the decay

products and the direction of the spin axis. The charged lepton or d-type quark from the W-boson decay have the highest correlations to the top quark spin axis. If we use these correlations to divide the data into a spin "up" and spin "down" component for the top quark, we can observe a difference between these two data sets in the angular correlations between the anti-top spin axis and the direction of motion of the anti-top decay products. For a "loose" set of cuts, we find that the difference between the correlations for the spin "up" verses spin "down" data samples can be as large as 25% at the Tevatron and 14% at the LHC, making these effects potentially observable. If the top quark is strongly coupled to new physics beyond the Standard Model, then these correlations could be dramatically altered.

ACKNOWLEDGMENTS

The Fermi National Accelerator Laboratory is operated by Universities Research Association, Inc., under contract DE-AC02-76CHO3000 with the U.S. Department of Energy. High energy physics research at the University of Michigan is supported in part by the U.S. Department of Energy, under contract DE-FG02-95ER40899. SP would like to thank T. Liss, R. Raja, A. Tollestrup and G. P. Yeh for valuable discussions. GDM would like to thank the Aspen Center for Physics, where a portion of this work was completed.

APPENDIX: SPINOR HELICITY BASIS FOR MASSIVE FERMIONS

In this appendix, we discuss the spinor helicity basis for massive fermions used to derive many of the results contained in this paper. This appendix follows the conventions and notation used in the review by Mangano and Parke [25], and is a very useful extension to that review. The connection to the spin state methods found in Bjorken and Drell [26] (Bj&D) is also included.

For a massive particle of momentum P and mass M, we follow Kleiss and Stirling [27] and pick a reference vector, p_2, which is lightlike, $p_2^2 = 0$. Usually it is convenient to choose p_2 as one of the massless particles in the situation under consideration. As we shall see later, the direction opposite to the spatial momentum of p_2 in the rest frame of the massive particle defines the axis along which the spin of the massive particle is decomposed. Then we define the vector p_1 by $p_1 = P - \frac{M^2}{2P\cdot p_2}\, p_2$. Note that p_1 is also a massless vector, $p_1^2 = 0$, and that

$$P = p_1 + \frac{M^2}{2p_1 \cdot p_2} p_2. \tag{A1}$$

For some applications it is convenient to rescale p_2 so that $P = p_1 + p_2'$, where $p_2' = \frac{M^2}{2p_1\cdot p_2}\, p_2$.

To obtain the spinors which are eigenstates of spin for the massive particle, we need to define two complex square roots of the factor $\frac{M^2}{2p_1\cdot p_2}$ by

$$\alpha \equiv \frac{M}{\langle p_1 - | p_2 + \rangle}, \qquad \beta \equiv \frac{M}{\langle p_2 + | p_1 - \rangle}. \tag{A2}$$

With these definitions $\alpha\beta = \frac{M^2}{2p_1\cdot p_2}$.

Then, the basis spinors describing the massive particle spin states are

$$u_\uparrow(P) = |p_1+\rangle - \beta\ |p_2-\rangle \qquad u_\downarrow(P) = |p_1-\rangle + \alpha\ |p_2+\rangle \tag{A3}$$

$$v_\uparrow(P) = |p_1-\rangle - \alpha\ |p_2+\rangle \qquad v_\downarrow(P) = |p_1+\rangle + \beta\ |p_2-\rangle \tag{A4}$$

$$\bar{u}_\uparrow(P) = \langle p_1 + | - \alpha\ \langle p_2 - | \qquad \bar{u}_\downarrow(P) = \langle p_1 - | + \beta\ \langle p_2 + | \tag{A5}$$

$$\bar{v}_\uparrow(P) = \langle p_1 - | - \beta\ \langle p_2 + | \qquad \bar{v}_\downarrow(P) = \langle p_1 + | + \alpha\ \langle p_2 - | \,. \tag{A6}$$

As expected, the spin states are a superposition of the two possible chiralities. They satisfy all the usual relations:

the Dirac equations

$$(\not{P} - M)u(P) = 0, \qquad \bar{u}(P)(\not{P} - M) = 0, \tag{A7}$$

$$(\not{P} + M)v(P) = 0, \qquad \bar{v}(P)(\not{P} + M) = 0, \tag{A8}$$

the completeness conditions

$$\sum_\lambda u_\lambda(P)\bar{u}_\lambda(P) = \not{P} + M, \qquad \sum_\lambda v_\lambda(P)\bar{v}_\lambda(P) = \not{P} - M, \tag{A9}$$

and the orthogonality conditions

$$\bar{u}_{\lambda_1}(P)u_{\lambda_2}(P) = 2M\delta_{\lambda_1,\lambda_2}, \qquad \bar{v}_{\lambda_1}(P)v_{\lambda_2}(P) = -2M\delta_{\lambda_1,\lambda_2}, \tag{A10}$$

$$\bar{u}_{\lambda_1}(P)v_{\lambda_2}(P) = 0, \qquad \bar{v}_{\lambda_1}(P)u_{\lambda_2}(P) = 0. \tag{A11}$$

To make contact with the methods of Bj&D for massive fermion states, we must first make trivial modifications to account for Bj&D's choice of normalization. Instead of decomposing the particle's momentum, however, Bj&D make use of a vector s, which satisfies

$$s^2 = -1, \quad P \cdot s = 0. \tag{A12}$$

In the particle's rest frame, the spatial part of s points in the same direction as the particle's spin. The relation between the two descriptions is provided by the following identities

$$p_1 = \frac{P + Ms}{2}, \qquad \frac{M^2}{2p_1 \cdot p_2}p_2 = \frac{P - Ms}{2}. \tag{A13}$$

To see that this is indeed correct, evaluate some outer products $u\bar{u}$ or $v\bar{v}$ for some spin projection using our spinors, make the above substitutions, and you will recover the Bj&D expressions, *e.g.* $u(P,s)\bar{u}(P,s) = \frac{1}{2}(\not{P} + M)(1 + \gamma_5 \not{s})$.

To describe the spin direction in terms of p_2, we invert (A13), and evaluate the resulting expression in the rest frame of the massive particle, where p_2 points in the direction of some unit vector $\hat{\mathbf{n}}$. For $P = (M, \vec{0})$ and $p_2 = (1, \hat{\mathbf{n}})$ we obtain $s = (0, -\hat{\mathbf{n}})$. Therefore,

the direction of the particle's spin is *opposite* to the direction of the spatial part of p_2 [28]. Alternatively, the particle's spin is in the *same* direction as the spatial part of p_1 in the massive particle's rest frame.

Next, we consider eigenstates of helicity. Since helicity is simply the spin projected along the direction of motion of the particle, choose $p_2 = p(1, -\hat{\mathbf{n}})$ for a massive particle with momentum $P = (\sqrt{p^2 + M^2}, p\,\hat{\mathbf{n}})$. Then,

$$p_1 = \frac{\sqrt{p^2 + M^2} + p}{2}\,(1, \hat{\mathbf{n}}) \tag{A14}$$

$$\frac{M^2}{2p_1 \cdot p_2}\,p_2 = \frac{\sqrt{p^2 + M^2} - p}{2}\,(1, -\hat{\mathbf{n}}). \tag{A15}$$

It is conventional to label these helicity states by "L" and "R", instead of "$\downarrow$" and "$\uparrow$" respectively.

In the large momentum limit,

$$p_1 \to P, \qquad \frac{M^2}{2p_1 \cdot p_2}\,p_2 \to 0. \tag{A16}$$

Therefore the basis spinors (A3)–(A6) become pure chirality eigenstates:

$$u_{\mathrm{R}}(P) \to |p_1+\rangle \quad u_{\mathrm{L}}(P) \to |p_1-\rangle \tag{A17}$$

$$v_{\mathrm{R}}(P) \to |p_1-\rangle \quad v_{\mathrm{L}}(P) \to |p_1+\rangle \tag{A18}$$

$$\bar{u}_{\mathrm{R}}(P) \to \langle p_1 +| \quad \bar{u}_{\mathrm{L}}(P) \to \langle p_1 -| \tag{A19}$$

$$\bar{v}_{\mathrm{R}}(P) \to \langle p_1 -| \quad \bar{v}_{\mathrm{L}}(P) \to \langle p_1 +|\,. \tag{A20}$$

Thus, in what is equivalent to the massless limit, the right-handed helicity state u_{R} becomes a state of pure right-handed chirality. That the right-handed helicity state v_{R} becomes a state of pure *left*-handed chirality simply reflects the fact that the helicity and chirality eigenvalues are *opposite* in sign for the anti-particle.

REFERENCES

* Electronic address: mahlon@umich.edu

† Electronic address: parke@fnal.gov

[1] F. Abe, *et. al.*, Phys. Rev. Lett. **74**, 2626 (1995).

[2] S. Abachi, *et. al.*, Phys. Rev. Lett. **74**, 2632 (1995).

[3] I. Bigi, Y. Dokshitzer, V. Khoze, J. Kühn, and P. Zerwas, Phys. Lett. **181B**, 157 (1986).

[4] V. Barger, J. Ohnemus, and R.J.N. Phillips, Int. J. Mod. Phys. **A4**, 617 (1989).

[5] G.L. Kane, J. Pumplin, and W. Repko, Phys. Rev. Lett. **41**, 1689 (1978).

[6] G.L. Kane, G.A. Ladinsky, and C.–P. Yuan, Phys. Rev. **D45**, 124 (1992).

[7] C.R. Schmidt and M.E. Peskin, Phys. Rev. Lett. **69**, 410 (1992).

[8] D. Atwood, A. Aeppli, and A. Soni, Phys. Rev. Lett. **69**, 2754 (1992).

[9] Y. Hara, Prog. Theo. Phys. **86**, 779 (1991); T. Arens and L.M. Seghal, Phys. Lett. **B302**, 501 (1993); D. Chang, S.–C. Lee, and P. Turcotte, Report No. hep–ph/9508357 (1995); W. Bernreuther, A. Brandenburg, and P. Uwer, Report No. PITHA 95/26, hep-ph/9510300 (1995).

[10] W. Bernreuther and A. Brandenburg, Phys. Lett. **B314**, 104 (1993); A. Brandenburg and J.P. Ma, Phys. Lett. **B298**, 211 (1993); W. Bernreuther and A. Brandenburg, Phys. Rev. **D49**, 4481 (1994).

[11] M. Jeżabek and J.H. Kühn, Phys. Lett. **B329**, 317 (1994).

[12] M. Anselmino, P. Kroll, and B. Pire, Phys. Lett. **B167**, 113 (1986); D. Atwood and A. Soni, Phys. Rev. **D45**, 2405 (1992); G.L. Ladinsky, Phys. Rev. **D46**, 3789 (1992); erratum **D47**, 3086 (1993); C.–P. Yuan, Phys. Rev. **D45**, 782 (1992); T. Arens and L.M. Seghal, Nucl. Phys. **B393**, 46 (1993); J.G. Körner, A. Pilaftsis, and M.M. Tung,

Z. Phys. **C63**, 575 (1994); R. Harlande, M. Jeżabek, J.H. Kühn, and T. Teubner, Phys. Lett. **B346**, 137 (1995).

[13] C.A. Nelson, Phys. Rev. **D41**, 2805 (1990); W. Bernreuther, J.P. Ma, and T. Schröder, Phys. Lett. **B297**, 318 (1992); W. Bernreuther, O. Nachtmann, P. Overmann, and T. Schröder, Nucl. Phys. **B388** 53, (1992); erratum **B406**, 516 (1993); F. Cuypers and S.D. Rindani, Phys. Lett. **B343**, 333 (1995); P. Poulose, S.D. Rindani, Phys. Lett. **B349**, 379 (1995).

[14] V.S. Fadin, V.A. Khoze, and M.I. Kotskii, Z. Phys. **C64**, 45 (1994); W. Bernreuther, J.P. Ma, and B.H.J. McKellar, Phys. Rev. **D51**, 2475 (1995); B. Kamal, Z. Merebashvili, and A.P. Contogouris, Phys. Rev. **D51**, 4808 (1995).

[15] To make these results easier to read the slashes have been left off the momentum vectors in the traces.

[16] The other possibility, $t_1 \propto p_L$ and $\bar{t}_1 \propto p_L$, leads to a slightly smaller spin asymmetry, 75% compared to 80%.

[17] We use the structure functions found in P. Harriman, A. Martin, R. Roberts and W.J. Stirling, Phys. Rev. **D42**, 798 (1990).

[18] We first became aware of the size of the asymmetry in the helicity basis for the Tevatron from T. Stelzer via a private communication with T. Liss.

[19] Use of the "beamline" basis for the LHC produces only 58% like-spin pairs.

[20] By spherical decay we mean that the decay $t \to b\, W^+$ is spherical in the t rest frame. However, the subsequent decay of the W-boson has all of the Standard Model spin correlations included.

[21] G. P. Yeh, private communication.

[22] R. Kleiss and W. J. Stirling, Z. Phys. C **40**, 419 (1988).

[23] C. Hill and S. Parke, Phys. Rev. **D49**, 4454 (1994).

[24] E. Eichten and K. Lane, Phys. Lett. **B327**, 129 (1994).

[25] M. Mangano and S. Parke, Phys. Rep. **200**, 301 (1991).

[26] J. Bjorken and S. Drell, *Relativistic Quantum Mechanics* (McGraw-Hill Book Company, New York, 1964).

[27] R. Kleiss and W. J. Stirling, Nuc. Phys. **B262**, 235 (1985).

[28] None of above definitions depend on the sign of the energy component of any of the vectors. However, if the energy components of the massive particle and p_2 have opposite sign, then the spin axis is in the same direction as the spatial momentum of p_2.

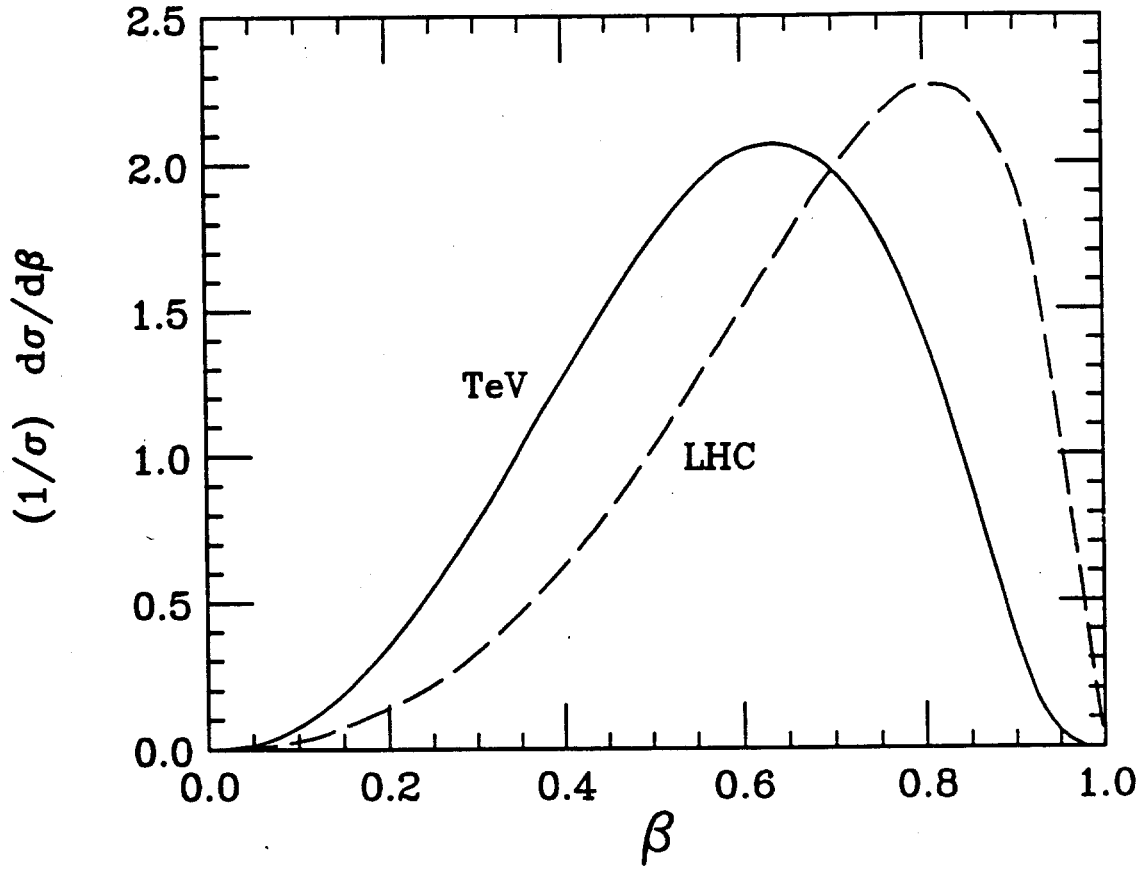

FIG. 1. Differential cross section for $t\bar{t}$ production as a function of the zero momentum frame speed β of the top quark for the 2.0 TeV Tevatron (solid) and 14 TeV LHC (dashed).

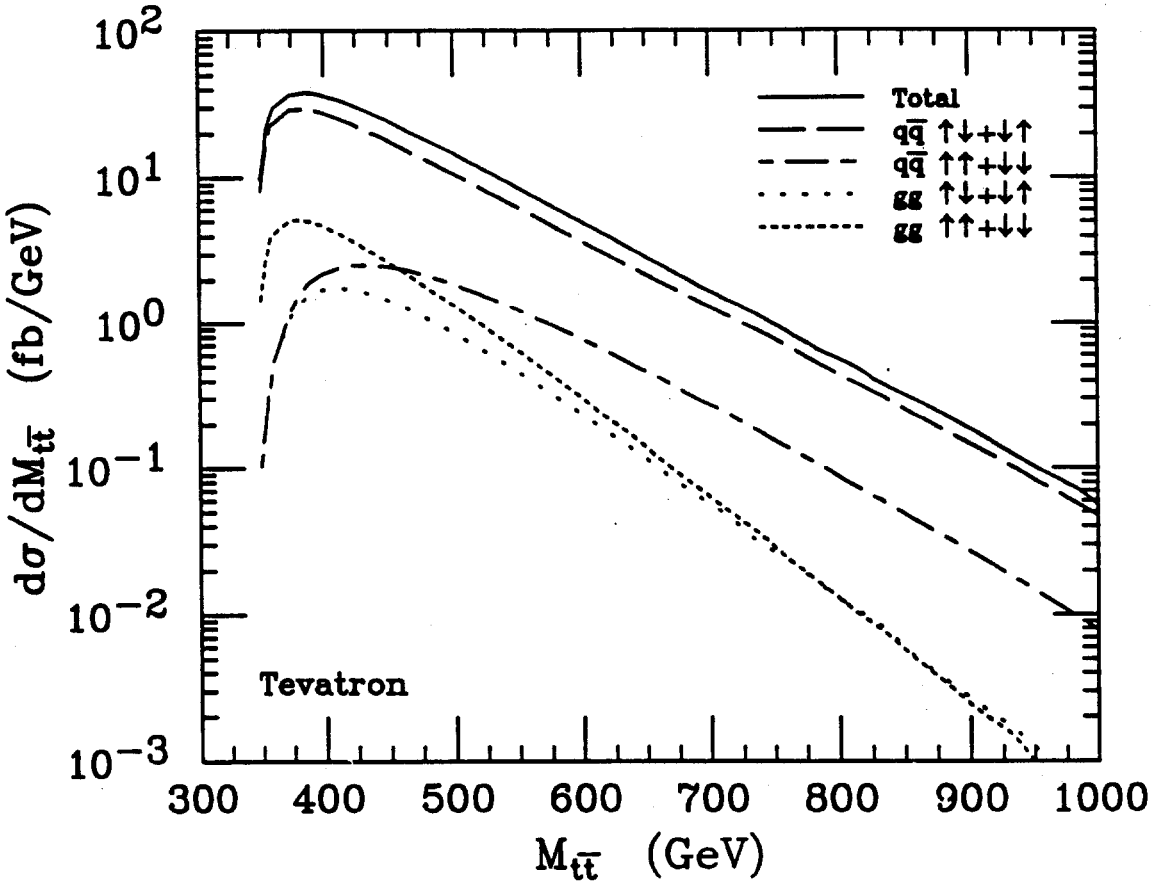

FIG. 2. Differential cross section for $t\bar{t}$ production as a function of the $t\bar{t}$ invariant mass, $M_{t\bar{t}}$, for the Tevatron with center of mass energy 2.0 TeV, decomposed into $\uparrow\downarrow+\downarrow\uparrow$ and $\uparrow\uparrow+\downarrow\downarrow$ spins of the $t\bar{t}$ pair using the "beamline" basis for both $q\bar{q}$ and gg components.

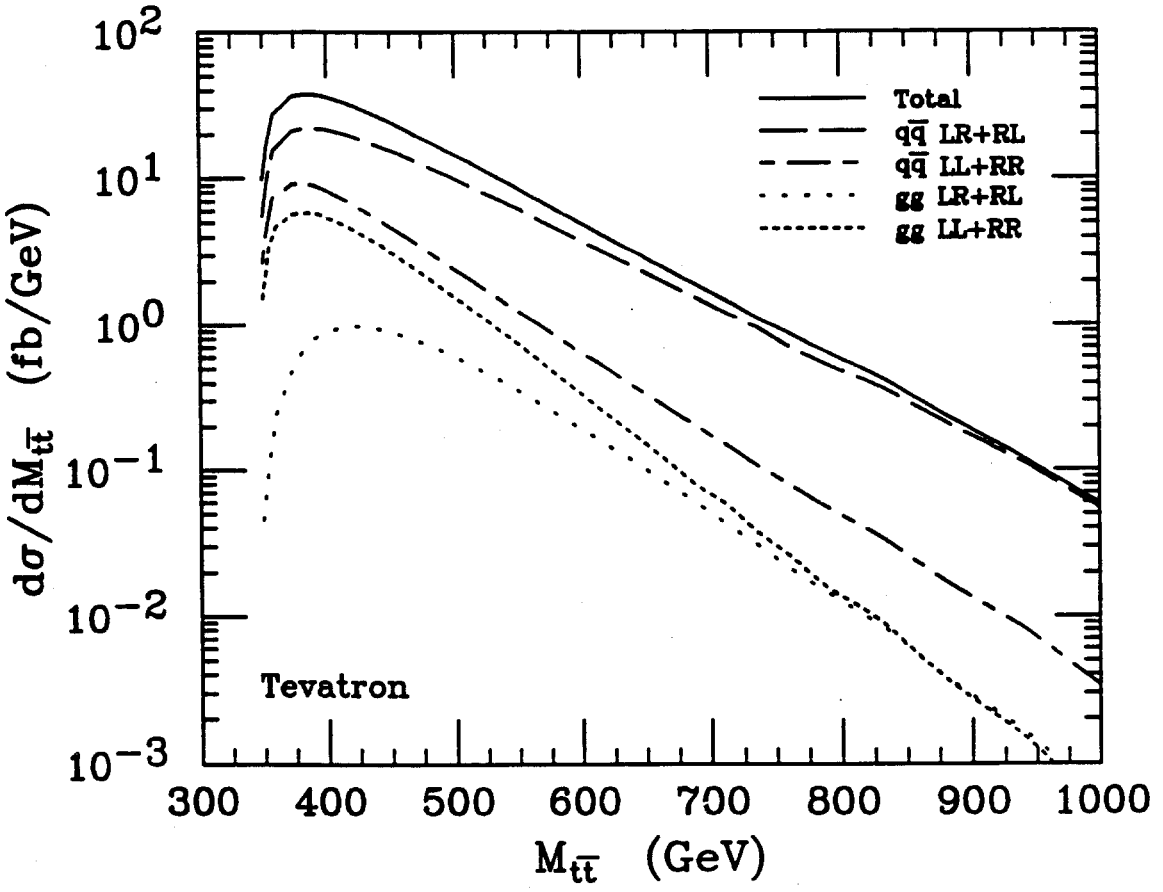

FIG. 3. Differential cross section for $t\bar{t}$ production as a function of the $t\bar{t}$ invariant mass, $M_{t\bar{t}}$, for the Tevatron with center of mass energy 2.0 TeV, decomposed into LR+RL and LL+RR helicities in the zero momentum frame of the $t\bar{t}$ pair for both $q\bar{q}$ and gg components.

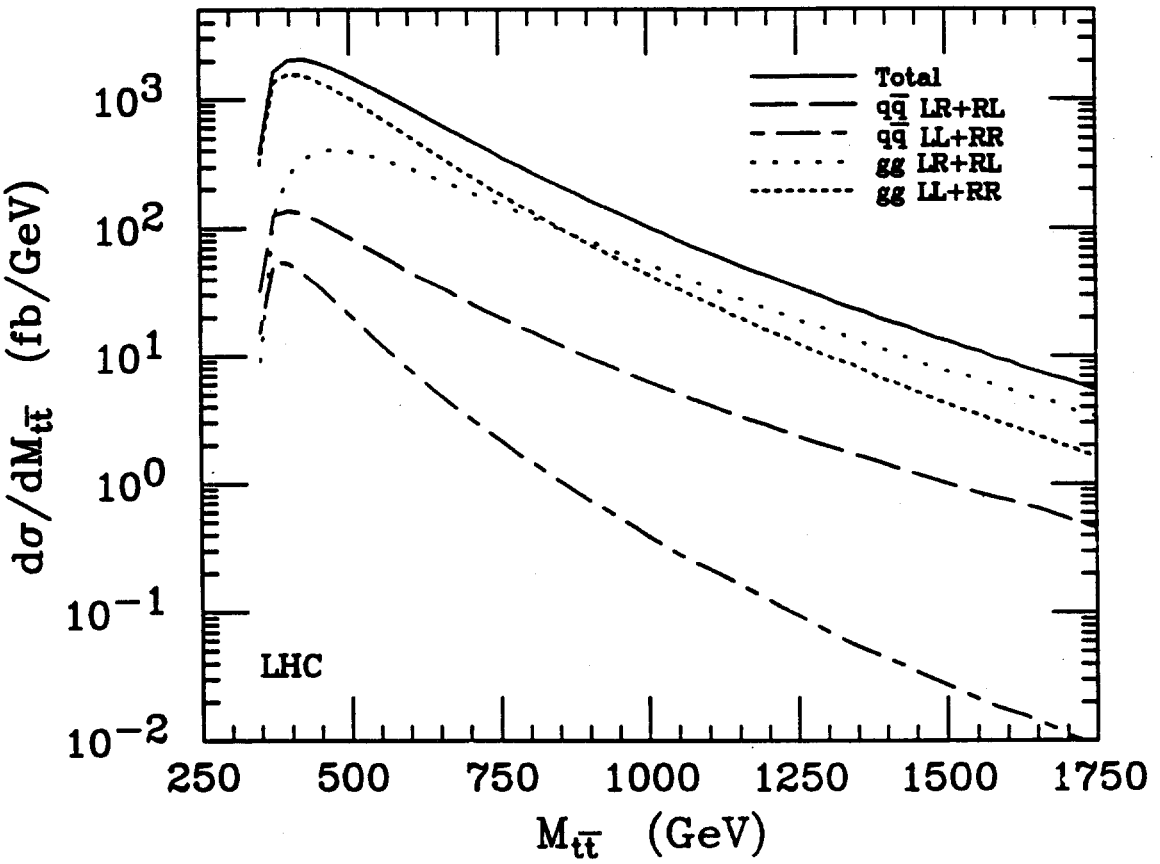

FIG. 4. Differential cross section for $t\bar{t}$ production as a function of the $t\bar{t}$ invariant mass, $M_{t\bar{t}}$, for the LHC with center of mass energy 14 TeV, decomposed into LR+RL and LL+RR helicities in the zero momentum frame of the $t\bar{t}$ pair for both $q\bar{q}$ and gg components.

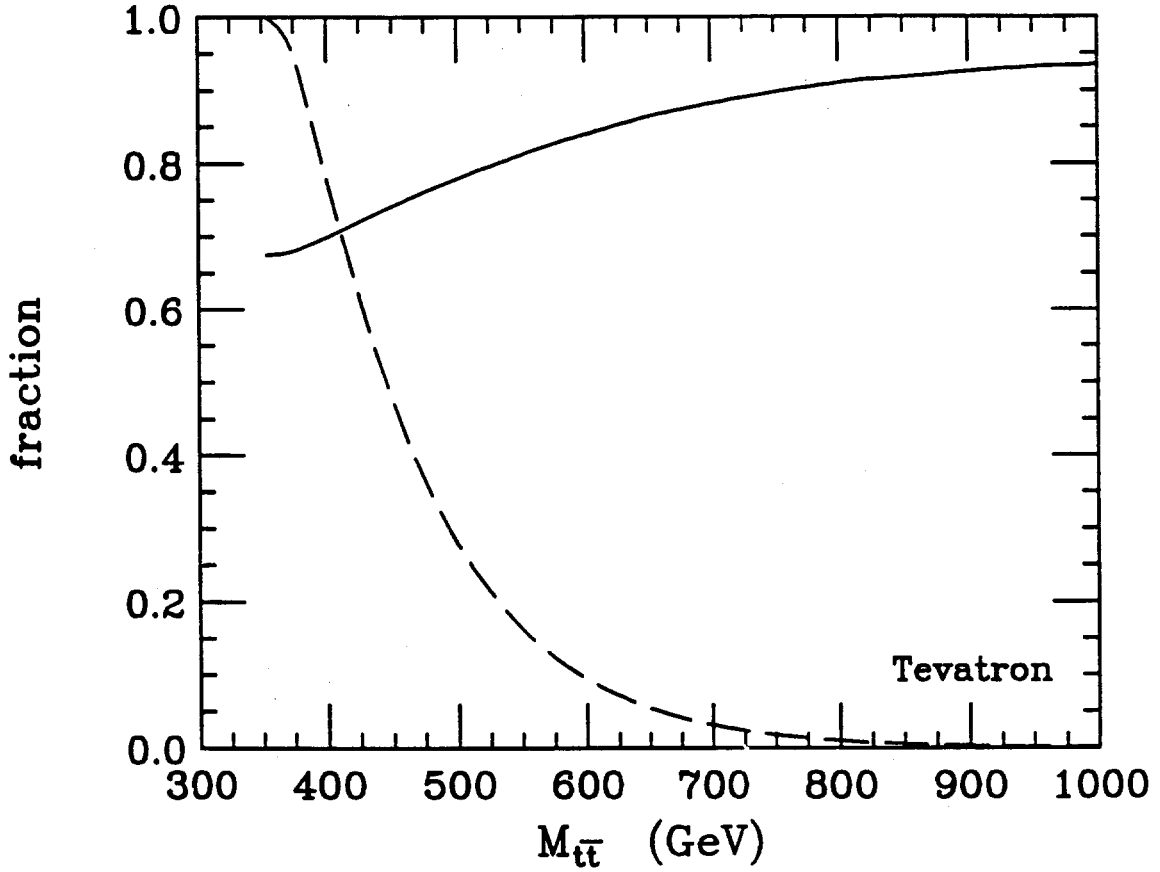

FIG. 5. The solid curve is the fraction of those $t\bar{t}$ pairs at the Tevatron (2.0 TeV) with an invariant mass *above* $M_{t\bar{t}}$ which have helicities LR+RL. The dashed curve is the fraction of the total cross section with an invariant mass *above* $M_{t\bar{t}}$.

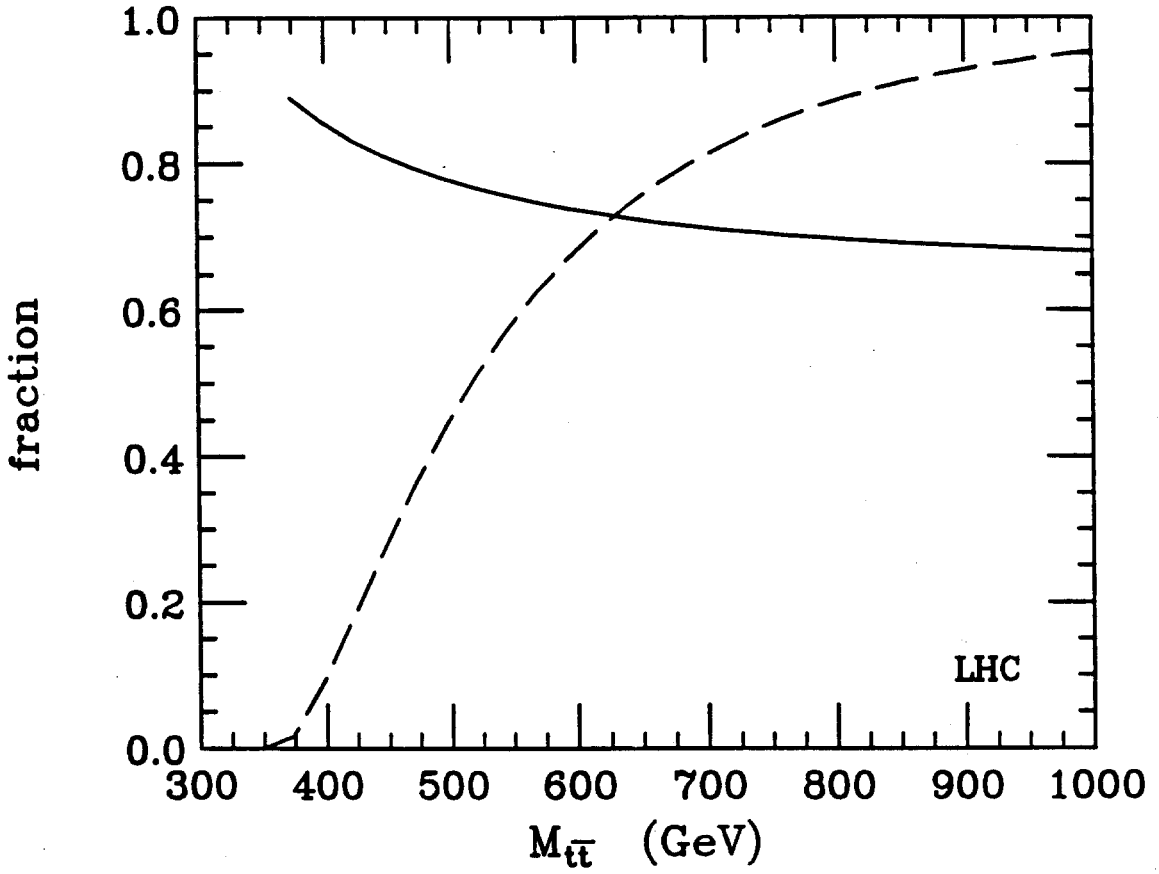

FIG. 6. The solid curve is the fraction of those $t\bar{t}$ pairs at the LHC (14 TeV) with an invariant mass *below* $M_{t\bar{t}}$ which have helicities LL+RR. The dashed curve is the fraction of the total cross section with an invariant mass *below* $M_{t\bar{t}}$.

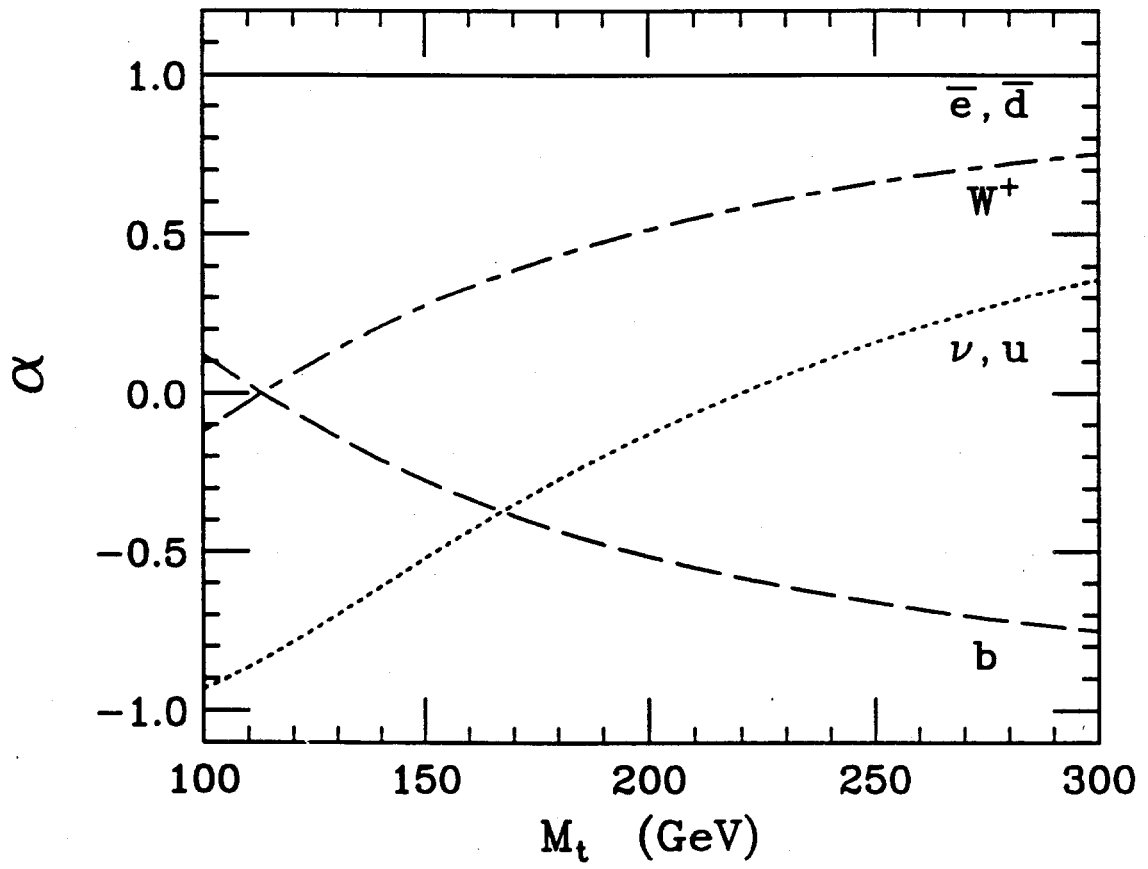

FIG. 7. Correlation coefficients, α_i, for a spin up top quark as a function of m_t, see Table I.

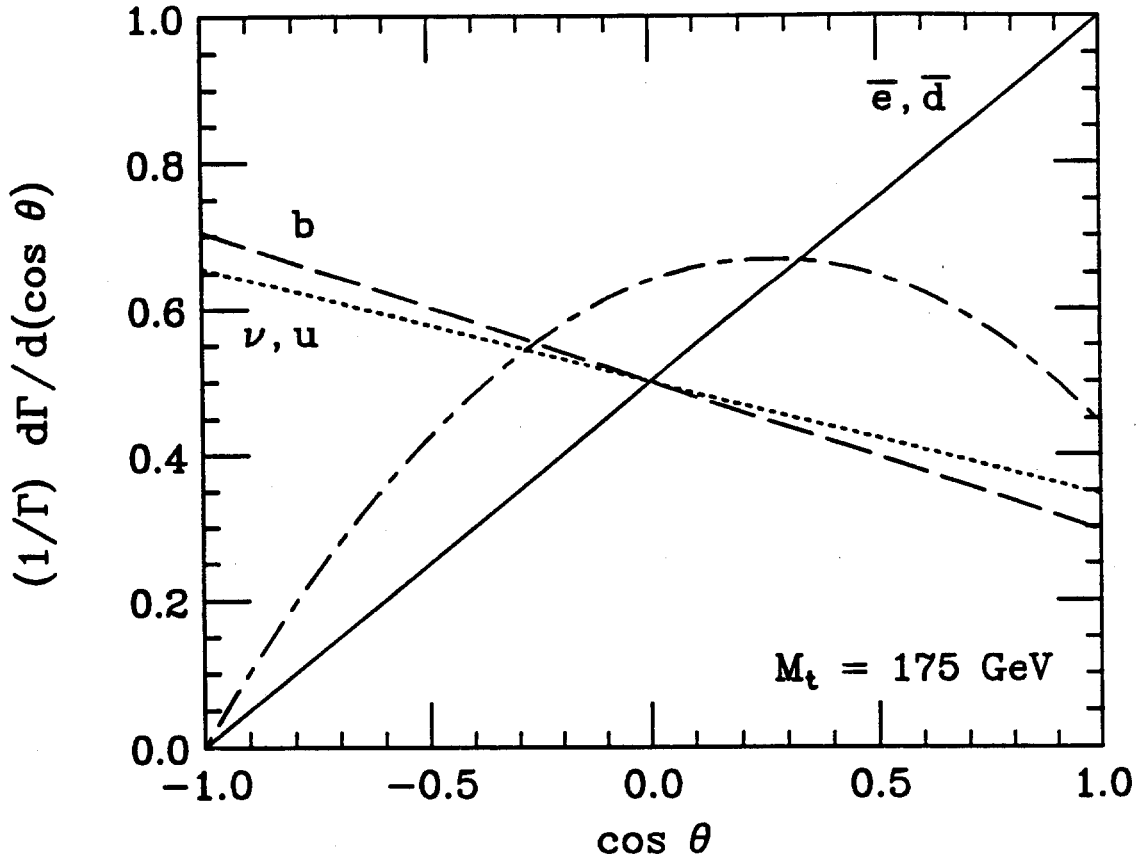

FIG. 8. Angular correlations in the decay of a 175 GeV spin-up top quark. The lines labelled $\bar{e}$, $\bar{d}$, b, ν and u are the angle between the spin axis and the particle in the rest frame of the top quark. The unlabelled dot-dash line is the angle between the b quark and the $\bar{e}$ or $\bar{d}$ in the rest frame of the W-boson.

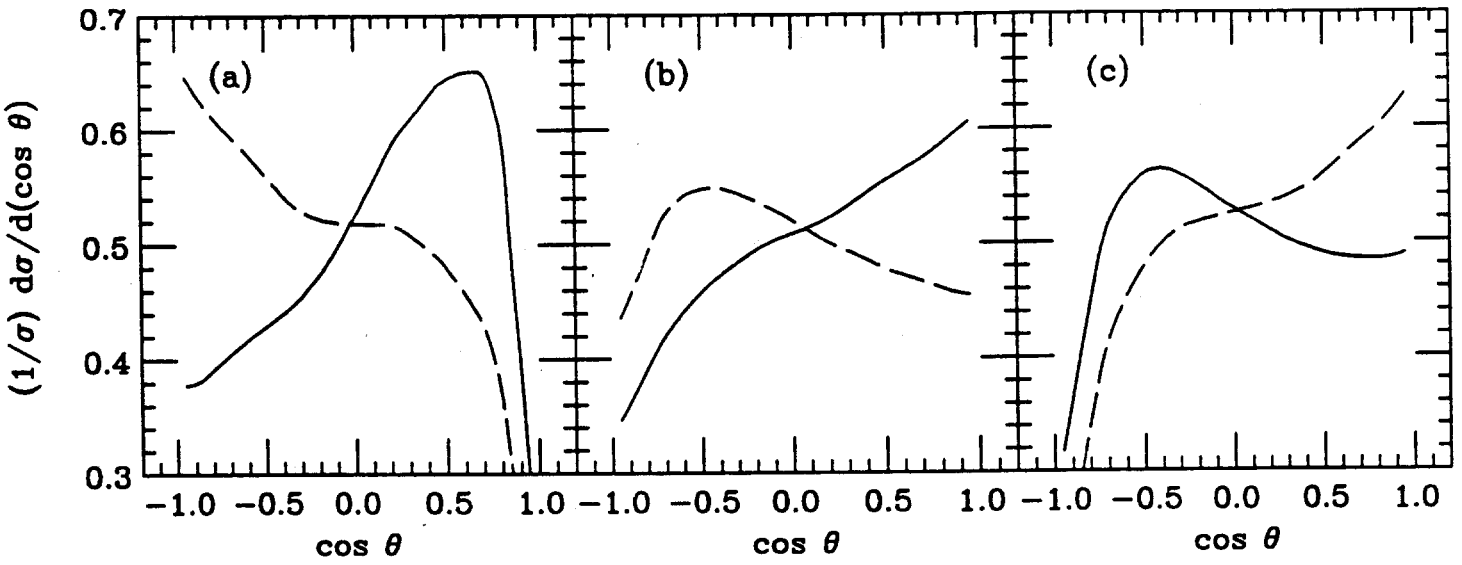

FIG. 9. Angular correlation between the two charged leptons in $t\bar{t}$ production and decay. Plotted is the angle between the charged lepton on the anti-top side of the event and the $\bar{t}$ spin axis in the $\bar{t}$ rest frame. The data are divided into spin-"up" (solid) and spin-"down" (dashed) top quark components, as determined from the charged lepton on the top side of the event for (a) the Tevatron using the "beamline" basis, (b) the Tevatron using the helicity basis, and (c) the LHC using the helicity basis.

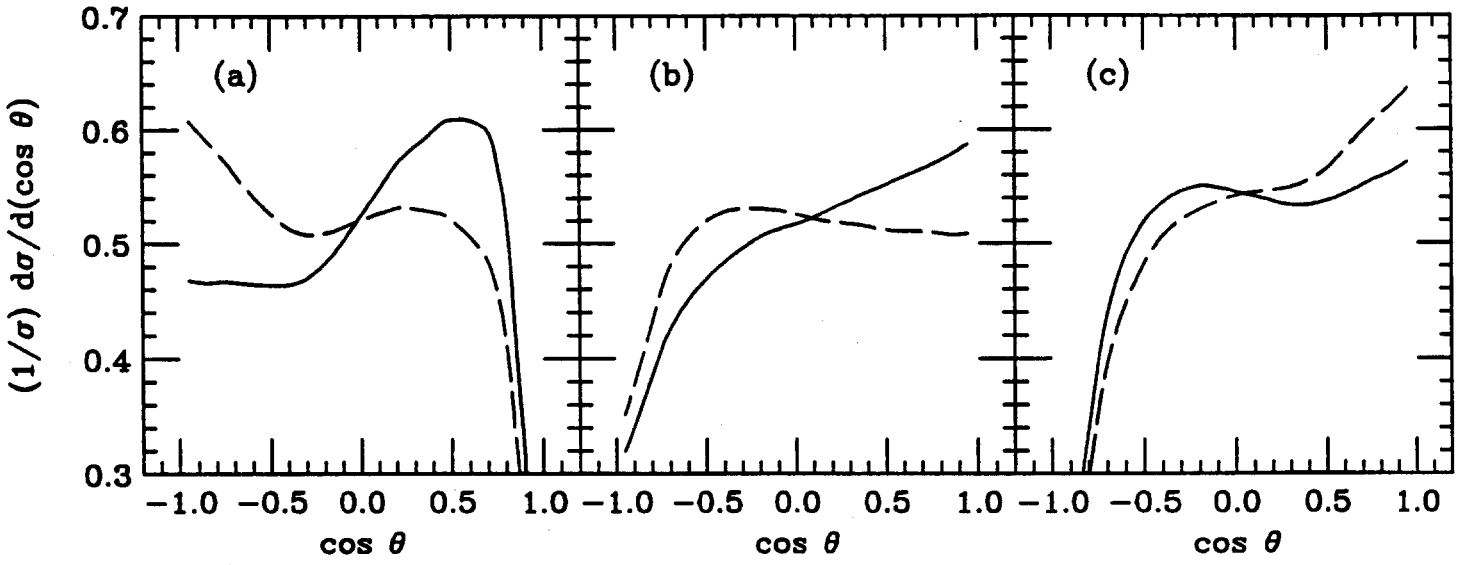

FIG. 10. Angular correlation between the charged lepton and the *"d"*-type quark in $t\bar{t}$ production and decay. Plotted is the angle between the *"d"*-type quark on the anti-top side of the event and the $\bar{t}$ spin axis in the $\bar{t}$ rest frame. The data are divided into spin-"up" (solid) and spin-"down" (dashed) top quark components, as determined from the charged lepton on the top side of the event for (a) the Tevatron using the "beamline" basis, (b) the Tevatron using the helicity basis, and (c) the LHC using the helicity basis.

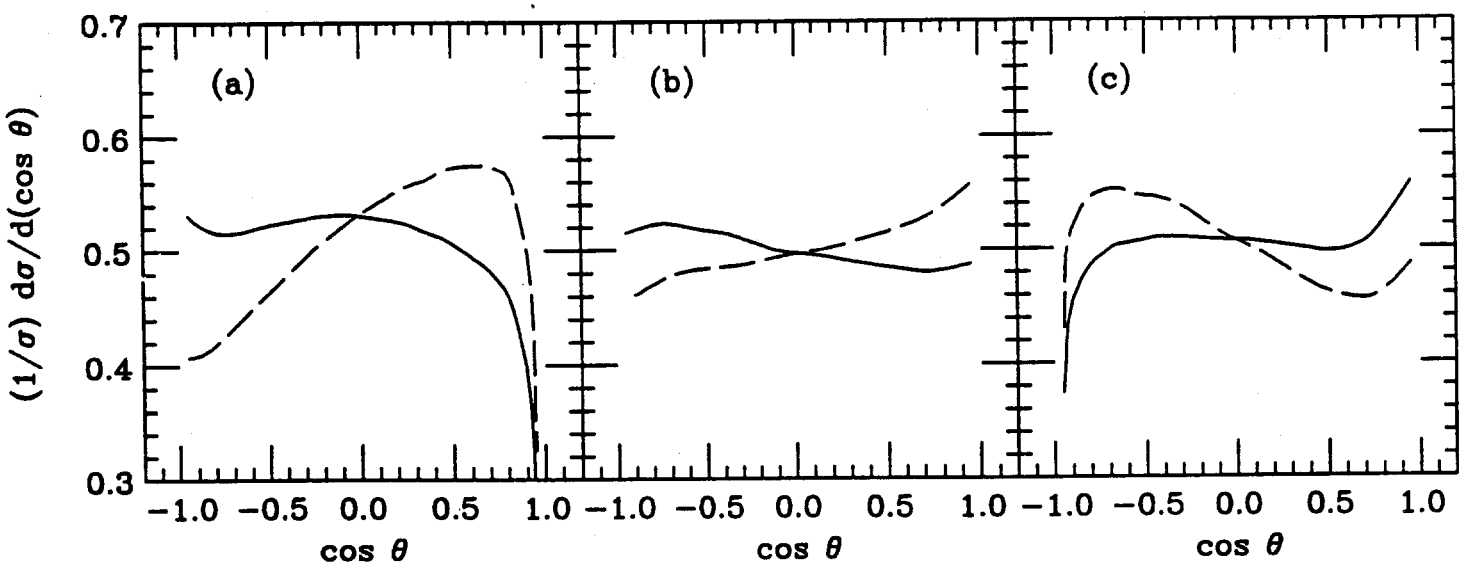

FIG. 11. Angular correlation between the charged lepton and the $\bar{b}$-quark in $t\bar{t}$ production and decay. Plotted is the angle between the $\bar{b}$-quark and the $\bar{t}$ spin axis in the $\bar{t}$ rest frame. The data are divided into spin-"up" (solid) and spin-"down" (dashed) top quark components, as determined from the charged lepton on the top side of the event for (a) the Tevatron using the "beamline" basis, (b) the Tevatron using the helicity basis, and (c) the LHC using the helicity basis.

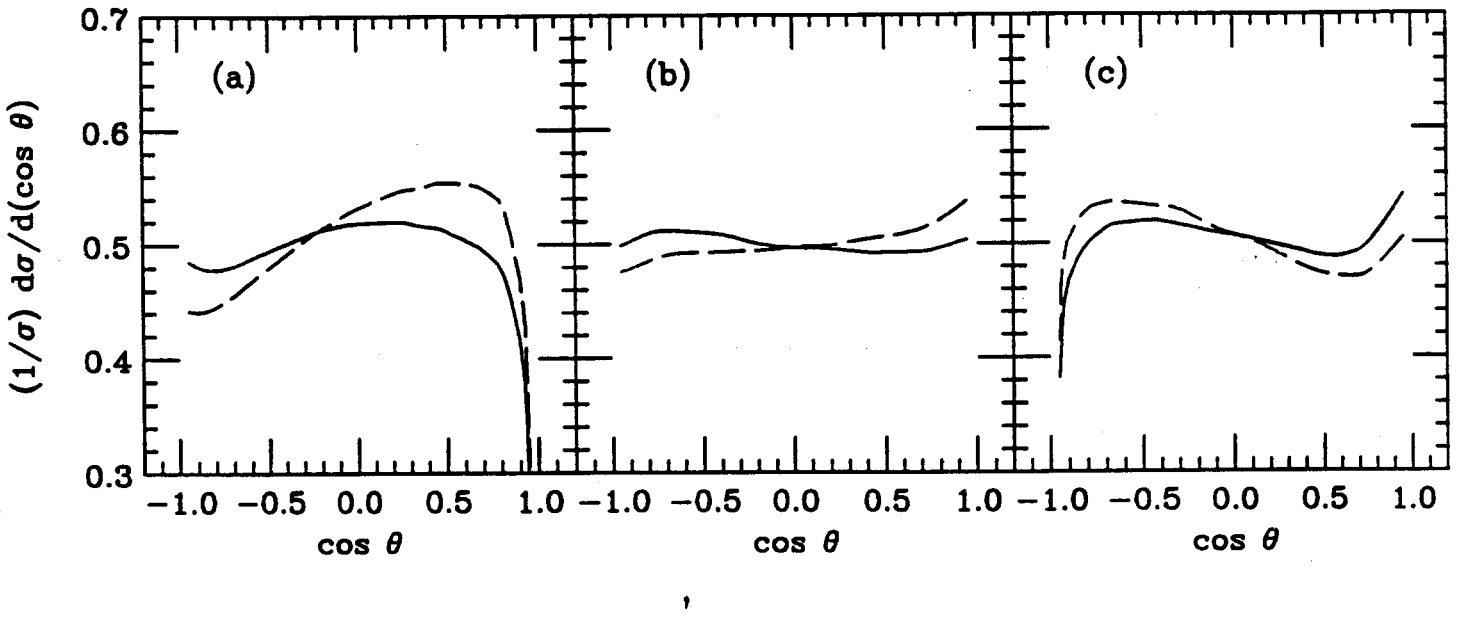

FIG. 12. Angular correlation between the two b-quarks in $t\bar{t}$ production and decay. Plotted is the angle between the $\bar{b}$-quark and the $\bar{t}$ spin axis in the $\bar{t}$ rest frame. The data are divided into spin-"up" (solid) and spin-"down" (dashed) top quark components, as determined from the b-quark on the top side of the event for (a) the Tevatron using the "beamline" basis, (b) the Tevatron using the helicity basis, and (c) the LHC using the helicity basis.

TABLES

TABLE I. Correlation coefficients α for both semi-leptonic and hadronic top quark decays as a function of $\xi \equiv m_t^2/m_w^2$ in the narrow width approximation for the W-boson and using $m_b = 0$. For $m_t > 100$ GeV these are excellent approximations.

$\bar{e}$ or $\bar{d}$	1
ν or u	$\dfrac{(\xi-1)(\xi^2-11\xi-2)+12\xi\ln\xi}{(\xi+2)(\xi-1)^2}$
W^+	$\dfrac{\xi-2}{\xi+2}$
b	$-\dfrac{\xi-2}{\xi+2}$

TABLE II. Predicted slopes of the *no cut* straight lines from Eq. (4.3) for the spin-"up" component of the angular distributions presented in Figs. 9–12.

top quark decay product	anti-top quark decay product	Tevatron ("beamline")	Tevatron (helicity)	LHC (helicity)
charged lepton	charged lepton	0.30	0.17	−0.17
charged lepton	"d"-type quark	0.15	0.085	−0.082
charged lepton	$\bar{b}$-quark	−0.12	−0.072	0.069
b-quark	$\bar{b}$-quark	−0.051	−0.029	0.028